

# Path-integral diffusion Monte Carlo: Calculation of observables of many-body systems in the ground state

Balázs Hetényi, Eran Rabani, and B. J. Berne

*Department of Chemistry and Center for Biomolecular Simulation, Columbia University, New York, New York 10027*

(Received 24 November 1998; accepted 4 January 1999)

We propose a new method to calculate ground state position dependent observables in quantum many-body systems. The method, which we call the path-integral diffusion Monte Carlo (PI-DMC) method, is essentially a combination of path-integral Monte Carlo (PIMC) and diffusion Monte Carlo (DMC) methods. The distribution resulting from a DMC simulation is further propagated in imaginary time by PIMC sampling. Tests of the new method for simple cases such as the harmonic oscillator, a double well, and a set of ten coupled harmonic oscillators show that the results for several observables converge rapidly to the exact result. © 1999 American Institute of Physics. [S0021-9606(99)51313-5]

## I. INTRODUCTION

Ground state properties of quantum many body systems are difficult to calculate. Ceperley and Kalos<sup>1</sup> present a review of the two most common approaches for computing ground state observables. One method is based on a variational formalism, where the energy of a trial function with adjustable parameters is optimized and the expectation value of observable  $A$  is obtained by application of the Metropolis Monte Carlo method<sup>2</sup> to evaluate

$$\langle A \rangle = \frac{\int d\mathbf{x} |\Psi_T(\mathbf{x}, \mathbf{a})|^2 A(\mathbf{x})}{\int d\mathbf{x} |\Psi_T(\mathbf{x}, \mathbf{a})|^2}, \quad (1)$$

where  $\mathbf{x}$  denotes the coordinates of the system,  $\Psi_T(\mathbf{x}, \mathbf{a})$  is a trial function whose form is known, and  $\mathbf{a}$  are the adjustable parameters. A reasonable trial function is an essential ingredient of the method. The other method known as the Green's function Monte Carlo (GFMC) uses a guided random walk to successively apply the Green's function of the relevant Schrödinger equation to an initial distribution to obtain a distribution that approximates the ground state wave function.

A method that is closely related to GFMC is the diffusion Monte Carlo<sup>3-5</sup> method. In this method a Gaussian random walk and a birth-death process is used to propagate a distribution in imaginary time, so that the contribution from components other than the ground state vanish exponentially. Both GFMC and DMC provide a distribution consistent with the ground state wave function, and not the ground state wave function squared. For this reason, augmentations of the method are necessitated in the calculation of observables.

For small systems with a few degrees of freedom observables may be obtained by histogramming the wave function.<sup>6</sup> Another common technique is the descendent weighting technique.<sup>1,7</sup> This method is quite difficult to program, and is also not very helpful in the case of large systems, since the variance of the weight increases with the number of generations of the birth-death process.<sup>1</sup> Another

possibility is to linearly couple the desired observable to a field, calculate the ground state energy of the system at several values of the field, and calculate the slope of the energy vs the field at zero field by interpolation.<sup>8-10</sup> A problem with this method is that several DMC runs need to be performed to obtain a good estimate of the slope, and if more than one observable is sought, the whole process needs to be repeated for each observable.

A different approach may be taken by resorting to the standard path-integral Monte Carlo (PIMC) method.<sup>11-13</sup> The PIMC method is based on the path integral formulation of quantum statistical mechanics due to Feynman,<sup>14</sup> and is useful in obtaining many body quantum statistical averages at finite temperatures. If a simulation is performed at extremely low temperature, reasonable estimates of ground state properties may be obtained.<sup>15</sup> A major problem with this method is that as the temperature is lowered, the Trotter number has to be increased correspondingly, resulting in an increase in the computational effort.

In this paper we propose an interesting alternative to the above methods and one that allows for the direct calculation of ground state position dependent observables by combining DMC and PIMC. In this method path-integrals are used to propagate a trial function in imaginary time. The closer the trial function is to the ground state wave function, the smaller will be the amplitude of excited state contributions to the trial function and only a short imaginary time propagation should be needed to obtain results within a desired error bar. In our proposed method, the trial function is the distribution generated by a DMC run.

In Sec. II we derive a path integral approximation for the average of a coordinate dependent observable that is distributed according to the square of the ground state wave function. The ground state wave function is the result of the imaginary time propagation of a trial function by path integrals. We then describe the implementation of the DMC distribution as the trial function, as well as how to obtain observables by this method. In Sec. III we perform a series of

tests on our proposed method, by making use of analytic expressions for the exact<sup>14</sup> and the approximate<sup>16</sup> forms of the imaginary time propagator for the harmonic oscillator. We then apply our proposed numerical method to several simple model systems, namely the linear harmonic oscillator, the double well, and a set of ten coupled harmonic oscillators. Conclusions are presented in Sec. IV.

## II. METHOD

In this section we describe our method for calculating expectation values for quantum many body systems. The method is a hybrid between DMC and imaginary time PIMC. We first provide the general framework for obtaining observables by imaginary time PIMC. As an input, this method requires a trial function which will be determined from DMC as outlined in Sec. II B.

### A. Ground state observables and imaginary time path integral Monte Carlo

The expectation value of a coordinate dependent observable  $A(x)$  in the ground state is

$$\langle A \rangle = Q_g^{-1} \int d\tilde{x} |\Psi_g(\tilde{x})|^2 A(\tilde{x}), \quad (2)$$

where  $Q_g$  is the normalization factor

$$Q_g = \int d\tilde{x} |\Psi_g(\tilde{x})|^2, \quad (3)$$

$\tilde{x}$  denotes the coordinate of the system, and  $\Psi_g(\tilde{x})$  is the unnormalized ground state wave function. For notational simplicity we refer to a one-dimensional system, but the concepts are trivially generalizable to the many dimensional case. The notation  $Q_g$  for the normalization integral may seem somewhat misleading, since in most cases the statistical mechanical partition function has a similar notation. In what follows the normalization integral, however, plays a role similar to the partition function, thus enabling the use of Monte Carlo methods in the evaluation of observables.

We seek an expression amenable to PIMC evaluation for Eq. (2). Propagation of a wave function (for the moment arbitrary) to imaginary time  $\tau$  gives

$$|\Psi(\tau)\rangle = \exp(-\tau\hat{H})|\Psi(0)\rangle, \quad (4)$$

where  $\hat{H}$  is the Hamiltonian operator of the system,  $|\Psi(0)\rangle$  is the ket corresponding to the trial function, and  $|\Psi(\tau)\rangle$  is the ket resulting from the propagation. For future usage we introduce the quantity

$$Q(\tau) = \langle \Psi(\tau) | \Psi(\tau) \rangle = \int d\tilde{x} \langle \Psi(\tau) | \tilde{x} \rangle \langle \tilde{x} | \Psi(\tau) \rangle, \quad (5)$$

which obeys

$$\lim_{\tau \rightarrow \infty} Q(\tau) = Q_g. \quad (6)$$

Inserting a coordinate resolution of the identity operator in Eq. (4) and writing the whole expression in the coordinate representation we obtain

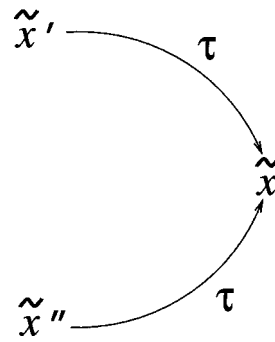


FIG. 1. Graphical representation of the integrand of Eq. (8).

$$\langle \tilde{x} | \Psi(\tau) \rangle = \int d\tilde{x}' \langle \tilde{x} | \exp(-\tau\hat{H}) | \tilde{x}' \rangle \langle \tilde{x}' | \Psi(0) \rangle, \quad (7)$$

which enables us to rewrite Eq. (5) as

$$Q(\tau) = \int d\tilde{x} \int d\tilde{x}' \int d\tilde{x}'' \langle \tilde{x}' | \exp(-\tau\hat{H}) | \tilde{x} \rangle \langle \tilde{x} | \exp(-\tau\hat{H}) | \tilde{x}'' \rangle \langle \tilde{x}' | \Psi(0) \rangle \langle \tilde{x}'' | \Psi(0) \rangle. \quad (8)$$

The expectation value of a coordinate dependent observable can now be expressed as

$$\begin{aligned} \langle A \rangle &= \lim_{\tau \rightarrow \infty} Q(\tau)^{-1} \int d\tilde{x} \int d\tilde{x}' \int d\tilde{x}'' A(\tilde{x}) \\ &\quad \times \langle \tilde{x}' | \exp(-\tau\hat{H}) | \tilde{x} \rangle \langle \tilde{x} | \exp(-\tau\hat{H}) | \tilde{x}'' \rangle \\ &\quad \times \langle \tilde{x}' | \Psi(0) \rangle \langle \tilde{x}'' | \Psi(0) \rangle. \end{aligned} \quad (9)$$

In essence the method we propose is to evaluate the average in Eq. (9) by sampling  $\tilde{x}$ ,  $\tilde{x}'$ , and  $\tilde{x}''$  using a real trial wave function at time  $\tau=0$ ,

$$\langle x | \Psi(0) \rangle = \Psi_T(x) \quad (10)$$

and a discrete imaginary time representation of the propagators. The integrand in Eq. (8) to be evaluated can be represented graphically as shown in Fig. 1.

In the standard PIMC method the kernel on the right-hand side of Eqs. (7) and (9) is split into  $p$  kernels each corresponding to imaginary time propagations of  $\tau/p$ . In the present application a slight generalization was required for reasons to be mentioned below, namely, we reserve the option of breaking up the imaginary time propagator unevenly (i.e., the imaginary time slices are not equal), which leads to

$$\begin{aligned} \langle \tilde{x} | \exp(-\tau\hat{H}) | \tilde{x}' \rangle &= \int \dots \int dx_2 \dots dx_p \\ &\quad \times \prod_{i=1}^p \langle x_i | \exp(-\epsilon_i \tau \hat{H}) | x_{i+1} \rangle, \end{aligned} \quad (11)$$

where  $x_1 = \tilde{x}$  and  $x_{p+1} = \tilde{x}'$  and  $\sum_{i=1}^p \epsilon_i = 1$ . The short imaginary time propagators may be symmetrically factorized into the approximate short time expression (Trotter breakup)

$$\begin{aligned} & \langle x_i | \exp(-\epsilon_i \tau \hat{H}) | x_{i+1} \rangle \\ & \approx \langle x_i | \exp(-\epsilon_i \tau \hat{T}) | x_{i+1} \rangle \\ & \quad \times \exp\left(-\frac{\epsilon_i \tau}{2}(V(x_i) + V(x_{i+1}))\right), \end{aligned} \quad (12)$$

where  $\hat{T}$  is the kinetic energy operator and  $V(x)$  is the potential energy at  $x$ . The error made in this approximation<sup>11,12,17</sup> can be shown to be proportional to  $(\epsilon_i \tau)^2$ . Inserting resolutions of the identity operator in the momentum representation in the kinetic energy kernel and integrating the momenta results in the standard short time (or high temperature) approximation<sup>11,12,17</sup> ubiquitous to many path integral based methods, i.e.,

$$\begin{aligned} & \langle x_i | \exp(-\epsilon_i \tau \hat{H}) | x_{i+1} \rangle \\ & \approx \left(\frac{m}{2\pi\tau\epsilon_i}\right)^{1/2} \exp\left(-\frac{m}{2\tau\epsilon_i}(x_i - x_{i+1})^2\right. \\ & \quad \left. - \frac{\epsilon_i \tau}{2}(V(x_i) + V(x_{i+1}))\right). \end{aligned} \quad (13)$$

Note that in the above we used atomic units and we shall do so throughout the paper.

Substituting Eq. (13) into Eq. (11), Eq. (11) into Eq. (7) and Eq. (7) into Eq. (5) we obtain the approximate expression

$$\begin{aligned} Q_p(\tau) &= \int d\tilde{x} \int \cdots \int dx_2 \cdots dx_{p+1} \int \cdots \int dx'_2 \cdots dx'_{p+1} \\ & \quad \times \prod_{i=1}^p \left(\frac{m}{2\pi\epsilon_i\tau}\right)^{1/2} \exp\left(-\frac{m}{2\epsilon_i\tau}(x_i - x_{i+1})^2\right. \\ & \quad \left. - \frac{\epsilon_i \tau}{2}(V(x_i) + V(x_{i+1}))\right) \Psi_T(\tilde{x}') \left(\frac{m}{2\pi\epsilon_i\tau}\right)^{1/2} \\ & \quad \times \exp\left(-\frac{m}{2\epsilon_i\tau}(x'_i - x'_{i+1})^2 - \frac{\epsilon_i \tau}{2}(V(x'_i)\right. \\ & \quad \left. + V(x'_{i+1}))\right) \Psi_T(\tilde{x}''), \end{aligned} \quad (14)$$

where  $\tilde{x} = x_1 = x'_1$ ,  $\tilde{x}' = x_{p+1}$ ,  $\tilde{x}'' = x'_{p+1}$  and the subscript  $p$  is meant as a reminder that this expression is the result of Trotter factorization. Defining

$$\begin{aligned} S_p(\tau, \mathbf{x}) &= \sum_{i=1}^p \frac{m}{2\epsilon_i\tau}(x_i - x_{i+1})^2 + \frac{\epsilon_i \tau}{2}(V(x_i) + V(x_{i+1})) \\ & \quad + \sum_{i=1}^p \frac{m}{2\epsilon_i\tau}(x'_i - x'_{i+1})^2 + \frac{\epsilon_i \tau}{2}(V(x'_i) + V(x'_{i+1})) \\ & \quad - \ln \Psi_T(x_{p+1}) - \ln \Psi_T(x'_{p+1}), \end{aligned} \quad (15)$$

where  $\mathbf{x}$  denotes collectively all the bead coordinates, for the average of a quantum observable we obtain

$$\langle A \rangle_p = \frac{\int \cdots \int d\mathbf{x} \exp(-S_p(\tau, \mathbf{x})) A(\tilde{x})}{\int \cdots \int d\mathbf{x} \exp(-S_p(\tau, \mathbf{x}))}. \quad (16)$$

The right-hand side of Eq. (14) is analogous to the statistical mechanical partition function of an open chain polymer with  $2p + 1$  monomers connected by harmonic springs. A similar analogy is exploited in the standard PIMC method. Other than the nearest neighbor harmonic potentials the intermediate beads<sup>18</sup> experience a potential proportional to  $V(x)$ , and the two terminal beads experience a potential proportional to  $V(x)$  plus a term that depends on the trial function [proportional to  $-\ln \Psi_T(x)$ ]. In the limit of long imaginary time [see Eq. (6)] and large<sup>19</sup>  $p$  the bead halfway along the chain (whose coordinate is denoted by  $\tilde{x}$ ) is distributed according to the square of the exact ground state wave function. In our method we evaluate coordinate dependent observables using the position of this bead, therefore from here on we will refer to it as the observation bead.

We have derived an expression [Eq. (16)] which is ideally suited for PIMC evaluation. The expression results from squaring a trial function propagated in imaginary time. A similar expression is given by Ceperley in Eq. (7.4) of Ref. 13 as a basis for the variational path integral (VPI) method. This method implements a trial function whose functional form is known such as the Jastrow wave function. As of yet the trial function in our method has been left arbitrary, but it would be advantageous to choose it such that it is close to the ground state. We now turn to address this issue.

## B. The trial function

For an arbitrary trial function care must be taken in choosing the value of  $\tau$  large enough to obtain a distribution sufficiently close to the ground state, but small enough for the simulation to be feasible. Runs with several values of  $\tau$  may be compared for convergence. Increasing  $\tau$  necessitates an increase in the discretization parameter  $p$ , and thus leads to a rise in computational effort. If, however, the trial function  $\Psi_T(x)$  is known to be close to the ground state wave function, shorter imaginary propagation time  $\tau$  (i.e., a smaller chain polymer) may be expected to provide sufficient results for the desired observable. Unfortunately, for an arbitrary system, the functional form of the ground state wave function is not known *a priori*. The DMC and GFMC methods, however, are both capable of providing a set of replicas of the system distributed in coordinate space according to the ground state wave function. Therefore we seek to implement a distribution generated by DMC (shall be denoted by  $\Psi_{\text{DMC}}(x)$ ) as the trial function in Eq. (16).

Given a trial function  $\Psi_T(x)$  the usual Monte Carlo algorithm can be constructed for the evaluation of Eq. (16) in which the positions of all the beads (including the terminal beads) are drawn from a uniform random distribution and the acceptance criterion is given by

$$\text{acc}(\mathbf{x}_{\text{old}} \rightarrow \mathbf{x}_{\text{new}}) = \min[1, \exp\{-\Delta S_p(\tau, \mathbf{x})\}], \quad (17)$$

where

$$\Delta S_p(\tau, \mathbf{x}) = S_p(\tau, \mathbf{x}_{\text{new}}) - S_p(\tau, \mathbf{x}_{\text{old}}), \quad (18)$$

where  $\mathbf{x}_{\text{old}}$  and  $\mathbf{x}_{\text{new}}$  denote the coordinates of the old and the new configurations respectively. If, however, we were able to draw the positions of the terminal beads from the distri-

bution  $\Psi_T(x)$  instead of a uniform random distribution, the acceptance criterion would have to be constructed using the modified action

$$S_p^{\text{mod}}(\tau, \mathbf{x}) = S_p(\tau, \mathbf{x}) + \ln \Psi_T(x_{p+1}) + \ln \Psi_T(x'_{p+1}), \quad (19)$$

leading to the acceptance criterion

$$\text{acc}(\mathbf{x}_{\text{old}} \rightarrow \mathbf{x}_{\text{new}}) = \min[1, \exp\{-\Delta S_p^{\text{mod}}(\tau, \mathbf{x})\}]. \quad (20)$$

Since the replicas obtained from a DMC simulation are distributed according to  $\Psi_{\text{DMC}}(x)$ , it is possible to draw the positions of the terminal beads from the distribution  $\Psi_{\text{DMC}}(x)$  without having to know its functional form. This procedure would effectively set

$$\Psi_T(x) = \Psi_{\text{DMC}}(x). \quad (21)$$

From a methodical point of view the above idea translates into the following:

- (1) After the DMC run reaches steady state, the replicas are stored in an array (number of coordinates  $\times$  number of replicas). These replicas are distributed according to the ground state wave function.
- (2) The positions of the two terminal beads are sampled from the distribution of replicas. This can be realized as follows: as an initial configuration, for each terminal bead we randomly choose a replica and place the terminal bead at the position of the chosen replica. A trial move in the terminal bead is made by randomly choosing a replica, and equating the positions of the terminal bead to the position of the newly chosen replica. In the case of many degrees of freedom, since a replica corresponds to a position in the overall configuration space of the system, the terminal bead corresponding to each coordinate needs to be moved simultaneously for such a trial move.
- (3) Accept or reject the proposed move based on the known part of the potential that the given terminal beads experience [i.e., the harmonic spring connecting it to the neighboring bead and  $\epsilon_{p+1}\tau V(x)/2$ ]. The term proportional to  $-\ln \Psi_T(x)$  is already taken into account, since we are drawing the positions of the terminal beads from a set of replicas which are distributed according to  $\Psi_T(x)$ .
- (4) The intermediate beads may be moved by standard PIMC methods.<sup>13</sup> We generalize the staging algorithm to make it suitable for the application presented here as described in Sec. II C.

In the case of many degrees of freedom a difficulty with the above prescription is that as the terminal beads are moved the harmonic springs attaching them to the neighboring beads on the chain may stretch enormously and these trial moves will often be rejected. This is the circumstance which inspired the uneven breakup of the imaginary time propagator. If the time slice that determines the spring constant of the spring connecting a terminal bead to the next bead ( $\epsilon_{p+1}$ ) is increased, then this spring becomes less stiff, hence the chain becomes more flexible. However since the error due to the breakup of the imaginary time propagator is proportional to  $(\epsilon_{p+1}\tau)^2$  increasing  $\epsilon_{p+1}$  will introduce er-

rors into the propagation. The introduced error can have components from the ground and excited states. Since the excited state components vanish upon imaginary time propagation, the increase in  $\epsilon_{p+1}$  may necessitate further imaginary time propagation by PIMC.

To further facilitate sampling the DMC wave function by the terminal beads, we also applied a neighbor list. As stated above trial moves of the terminal beads are accomplished by randomly choosing from the list of stored replicas. Instead of randomly choosing a replica, we set up a neighbor list for each replica (an array which for each replica stores the index of all the other replicas within some cutoff distance  $R_{\text{cut}}$ ), and trial moves are made by randomly choosing a replica from the neighbor list of the current replica.

The use of variable time slices and neighbor lists allowed efficient sampling of the terminal beads, and also control over the acceptance probability.

### C. Staging for an uneven polymer chain

A reduction in the computational effort for PIMC may be achieved by implementation of the staging transformation.<sup>20,21</sup> The idea is to partially or completely diagonalize the kinetic part of the action, and thus sampling may be performed in terms of coordinates which obey a Gaussian distribution. The Cartesian coordinates in which nearest neighbors are connected by stiff harmonic bonds often render straightforward sampling inefficient.

In this subsection, we give the general expressions of the identities that provide the basis of the staging algorithm for an uneven polymer chain. Since only the fundamental identities needed to be rederived, subsequent steps of the construction of such an algorithm will only be outlined here, details may be found in the work of Pollock and Ceperley<sup>20</sup> and of Tuckerman *et al.*<sup>21</sup>

We introduce the following notation for the part of the imaginary time propagator associated with the kinetic energy:

$$\rho_0(x_i, x_{i+1}; \epsilon_i \tau) = \left( \frac{m}{2\pi \epsilon_i \tau} \right)^{1/2} \exp\left( -\frac{m}{2\epsilon_i \tau} (x_i - x_{i+1})^2 \right). \quad (22)$$

One can now write the matrix element of the full propagator as

$$\langle x_i | \exp(-\epsilon_i \tau \hat{H}) | x_{i+1} \rangle = \exp\left( -\frac{\epsilon_i \tau}{2} V(x_i) \right) \rho_0(x_i, x_{i+1}; \epsilon_i \tau) \times \exp\left( -\frac{\epsilon_i \tau}{2} V(x_{i+1}) \right). \quad (23)$$

A sequence of kinetic energy imaginary time propagators may be written as

$$\prod_{k=1}^j \rho_0(x_k, x_{k+1}; \epsilon_k \tau) = \rho_0(x_1, x_{j+1}; \tilde{\epsilon}_j \tau) \prod_{k=1}^j \left( \frac{m_k}{2\pi \tau} \right)^{1/2} \times \exp\left( -\frac{m_k}{2\tau} (x_k - x_k^*)^2 \right), \quad (24)$$

where

$$\tilde{\epsilon}_j = \sum_{i=1}^j \epsilon_i, \quad (25)$$

$$m_k = m \frac{\tilde{\epsilon}_k}{\epsilon_{k-1} \epsilon_k}, \quad (26)$$

$$x_k^* = \frac{\tilde{\epsilon}_k x_1 + \epsilon_{k+1} x_{k+1}}{\tilde{\epsilon}_k}. \quad (27)$$

Equation (24) follows from the identity

$$\frac{\rho_0(x_1, x_k; \alpha) \rho_0(x_k, x_{k+1}; \beta)}{\rho_0(x_1, x_{k+1}; \alpha + \beta)} = \left( \frac{m(\alpha + \beta)}{2\pi\alpha\beta} \right)^{1/2} \exp\left( -\frac{m(\alpha + \beta)}{2\alpha\beta} (x_k - \tilde{x}_k)^2 \right), \quad (28)$$

where

$$\tilde{x}_k = \frac{\beta x_1 + \alpha x_{k+1}}{\alpha + \beta}. \quad (29)$$

In the staging algorithm, a set of consecutive beads are chosen for a proposed move. The move is proposed in terms of the staged coordinates for the chosen beads which in our case are defined as

$$u_k = x_k - x_k^*. \quad (30)$$

These coordinates are distributed according to a Gaussian distribution, which allows their direct sampling as is done in the standard staging algorithm.

#### D. Observables

The PI-DMC method is helpful mainly in evaluating the ground state expectation value of coordinate dependent observables. To evaluate them one simply averages the value of the function corresponding to the desired observable at the sampled coordinate(s) of the observation bead.

The kinetic energy may be evaluated via the quantum mechanical virial theorem<sup>22</sup> which states that for stationary states

$$\langle T \rangle = \left\langle \frac{\tilde{x}}{2} \frac{\partial V(\tilde{x})}{\partial \tilde{x}} \right\rangle. \quad (31)$$

For sufficient imaginary time propagation the observation bead is expected to be distributed according to the probability distribution obtained by squaring the ground state wave function (a stationary state). The virial theorem is thus applicable for the evaluation of the kinetic energy, since the virial is a coordinate dependent observable.

The total ground state energy may be calculated in two ways. One is to use the virial theorem and construct the following virial estimator:

$$\epsilon_{\text{vir}} = \frac{\tilde{x}}{2} \frac{\partial V(\tilde{x})}{\partial \tilde{x}} + V(\tilde{x}). \quad (32)$$

The virial estimator used here is distinct from the virial estimator used in PIMC simulations,<sup>23</sup> which is based on the classical version of the virial theorem.

Another estimator for the ground state energy may be constructed in a manner similar to that of the PIMC primitive estimator. We take an arbitrary function  $|\Psi(0)\rangle$  and propagate it to imaginary time  $\tau$ ,

$$|\Psi(\tau)\rangle = \exp(-\tau\hat{H})|\Psi(0)\rangle. \quad (33)$$

Expanding  $|\Psi(0)\rangle$  in terms of the eigenfunctions of  $\hat{H}$  and substituting into Eq. (33) results in

$$|\Psi(\tau)\rangle = \sum_{n=0}^{\infty} a_n \exp(-\tau E_n) |\phi_n\rangle, \quad (34)$$

where  $E_n$  denote the eigenvalues and  $|\phi_n\rangle$  denote the eigenfunctions of  $\hat{H}$ . Using the definition of  $Q(\tau)$  [Eq. (5)] it can easily be shown that

$$\lim_{\tau \rightarrow \infty} \left[ -\frac{1}{2} \frac{\partial \ln Q(\tau)}{\partial \tau} \right] = E_0, \quad (35)$$

where  $E_0$  is the ground state energy.

Equation (35) provides the basis for the construction of an energy estimator. Substituting our approximate  $Q(\tau)$  from Eq. (14) we obtain the primitive ground state energy estimator

$$\epsilon_{\text{prtm}} = \frac{p}{\tau} - \sum_{i=1}^p \frac{m}{4\epsilon_i \tau^2} (x_i - x_{i+1})^2 + \frac{\epsilon_i}{4} (V(x_i) + V(x_{i+1})) - \sum_{i=1}^p \frac{m}{4\epsilon_i \tau^2} (x'_i - x'_{i+1})^2 + \frac{\epsilon_i}{4} (V(x'_i) + V(x'_{i+1})). \quad (36)$$

### III. RESULTS

In the following, the PI-DMC method is applied to simple model systems, and the results are compared to results known analytically or simulations using other methods that have been thoroughly tested. In the case of the harmonic oscillator, we use known formulas for the analytical and the discretized propagator to test mainly the convergence of the method. On the numerical side, we run a DMC simulation for a fixed imaginary time (sufficient to obtain the ground state energy) and store replicas, which shall be used to represent the ground state wave function. Subsequently we calculate ground state observables from the obtained distribution by PIMC propagation to various imaginary times. We also examine the effect of varying the Trotter number  $p$  on the results.

#### A. One-dimensional harmonic oscillator

Although simple, and rather well understood, the harmonic oscillator provides a reasonable testing ground for new methods, since a more detailed investigation is permitted than in the case of more complex systems.

Since the imaginary time propagator may be solved analytically both for the exact<sup>14</sup> and the discretized<sup>16</sup> case, we may test the general idea of our proposed method by analytically performing propagations on chosen initial wave func-

tions. The exact imaginary time propagator for a one dimensional harmonic oscillator as given by Feynman<sup>14</sup> is

$$\langle x | \exp(-\tau \hat{H}) | x' \rangle = \left( \frac{m\omega}{2\pi \sinh(\omega\tau)} \right)^{1/2} \exp \left\{ -\frac{m\omega}{2 \sinh(\omega\tau)} \right. \\ \left. \times [(x^2 + x'^2) \cosh(\omega\tau) - 2xx'] \right\}, \quad (37)$$

where  $m$  and  $\omega$  denote mass and frequency, respectively, and  $\tau$  denotes the imaginary time of propagation. Its discretized approximate analog given by Schweizer *et al.*<sup>16</sup> for a propagator whose imaginary time of propagation  $\tau$  is divided up into  $p$  even time increments is

$$\langle x | \exp(-\tau \hat{H}) | x' \rangle \approx \left( \frac{mpA}{2\pi\tau} \right)^{1/2} \exp \left\{ -\frac{m\omega}{2} [B(x^2 + x'^2) \right. \\ \left. - 2Axx'] \right\}, \quad (38)$$

where

$$A = \left( \frac{p}{\omega\tau} \right) \frac{f^{p-1}(f^2-1)}{(f^{2p}-1)}, \quad (39)$$

$$B = \left( \frac{\omega\tau}{2p} \right) + \frac{p}{\omega\tau} \frac{(f-1)(f^{2p-1}+1)}{(f^{2p}-1)}. \quad (40)$$

In the above equations we have also used the relations

$$f = 1 + \frac{1}{2}R^2 + \frac{12}{R}(4+R^2)^{1/2} \quad (41)$$

and

$$R = \frac{\omega\tau}{p}. \quad (42)$$

We are thus able to test the effect of discretization on the propagator in our method. To this end we use the exact ground state wave function for the harmonic oscillator given by

$$\Psi(x) = \left( \frac{\pi}{m\omega} \right)^{1/4} \exp \left( -\frac{m\omega}{2} x^2 \right) \quad (43)$$

as an initial wave function in Eq. (9), and calculate the average potential. The ground state wave function propagated by the discretized propagator with Trotter parameter  $p$  to imaginary time  $\tau$  follows from Eqs. (7), (38), and (43),

$$\Psi(x, \tau) = \left( \frac{\pi}{m\omega \left( B - \frac{A^2}{B+1} \right)} \right)^{1/4} \\ \times \exp \left\{ -\frac{m\omega}{2} \left( B - \frac{A^2}{B+1} \right) x^2 \right\}. \quad (44)$$

In Fig. 2 we present the results of analytic propagation using the exact and the discretized version of the propagator for a harmonic oscillator with mass  $m=1$  and frequency  $\omega=1$ . The average potential is calculated. The results show that discretizing the propagator leads to an underestimation of the average potential. As  $p$  is increased convergence to the

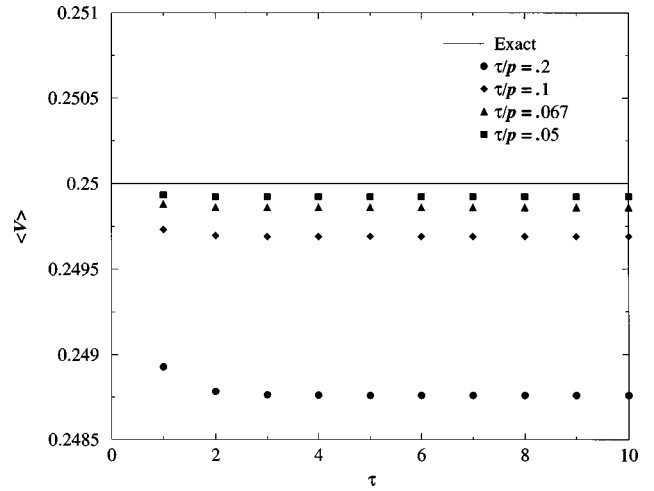


FIG. 2. Evaluation of the ground state potential energy of a linear harmonic oscillator as a function of propagation time  $\tau$  using the analytic form of the exact [see Eq. (37)] and the discretized [see Eq. (38)] propagator. The line corresponds to the exact propagator, the different symbols correspond to different factorizations (i.e., Trotter numbers).

known value of  $\langle V \rangle = 0.25$  is achieved. The conclusion that the average potential energy of a simple harmonic oscillator is underestimated by a discretized propagator also holds in the case of the standard finite temperature PIMC method,<sup>23</sup> where a cyclic chain is used in the algorithm. Note also that for short imaginary times, the results obtained by using the discretized propagator are closer to the exact result than for long imaginary times. This is due to the fact that we are propagating the exact ground state wave function, for which if the propagation time  $\tau$  was zero, then the exact result would be obtained.

The propagator given in Eq. (38) is for the case when the propagation time  $\tau$  is divided into equal increments. However in our method, the time slices are unequal [see Eq. (11)]. In the case of unequal breakup, Eq. (38) is no longer valid. Instead one can evaluate expectation values of propagated wave functions by evaluating the propagated wave function analytically at each imaginary time step and using the resulting wave function as the initial wave function for the next time step. The integrals one must evaluate in this case are all Gaussian, so the calculation may be done analytically. Since the functional form of the wave function is known at each time step, it can be used to calculate observables. The uneven time slices were defined such that the first propagation time step  $\tau_1$  is given a value, and the value of each subsequent time slice is given by the recursion formula

$$\tau_{i+1} = \tau_i/a, \quad (45)$$

where  $a$  is an input parameter. This recursion relation is followed until the first  $\tau_i \leq \delta$  is reached, then  $\tau_i$  is set equal to  $\delta$  and subsequently all  $\tau_i$  are set equal to  $\delta$ .

The results shown in Fig. 3 were obtained by setting  $a=2$ ,  $\delta=0.05$  and by varying the value of the initial time slice  $\tau_1$  from 0.25 to 0.5. We compare to the case of the even breakup where  $\tau/p=0.05$ . We find that the two propagations

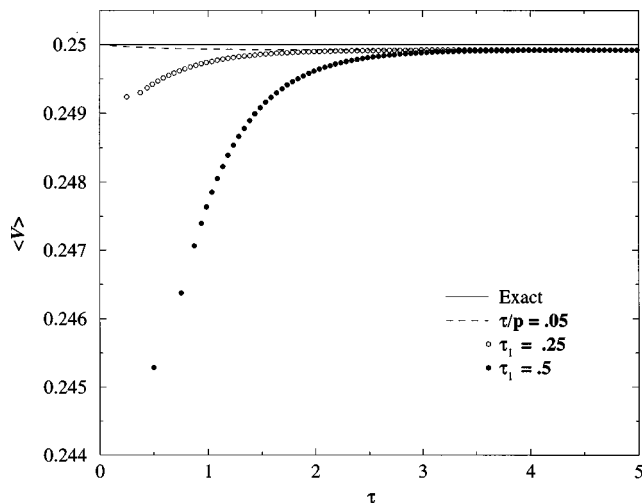


FIG. 3. Evaluation of the average potential energy of the linear harmonic oscillator as a function of propagation time  $\tau$  using the analytic form of the exact propagator [see Eq. (37)] and both the evenly discretized [see Eq. (38)] and unevenly discretized propagators [an expression for the wave function is given by Eq. (44)] for  $\tau_1=0.25$  and  $\tau_1=0.5$ . The solid line denotes the result using the exact propagator, the dashed line denotes the result using an evenly discretized propagator with  $\tau/p=0.05$ , the symbols denote the results of using unevenly discretized propagators with different initial times  $\tau_1$ .

using different initial times all converge in the limit of long imaginary time to the result obtained by the evenly divided propagator.

It is also instructive to assess the advantage of using the ground state wave function instead of some other trial function. By propagation of Gaussian trial functions of the form

$$\Psi(x) = \left( \frac{\pi}{\alpha m \omega} \right)^{1/4} \exp\left( -\frac{\alpha m \omega}{2} x^2 \right), \quad (46)$$

where  $\alpha$  is an input parameter ( $\alpha=1$  corresponds to the exact ground state wave function). The results are shown in Fig. 4 for three different values of  $\alpha$ . The exact propagator is used

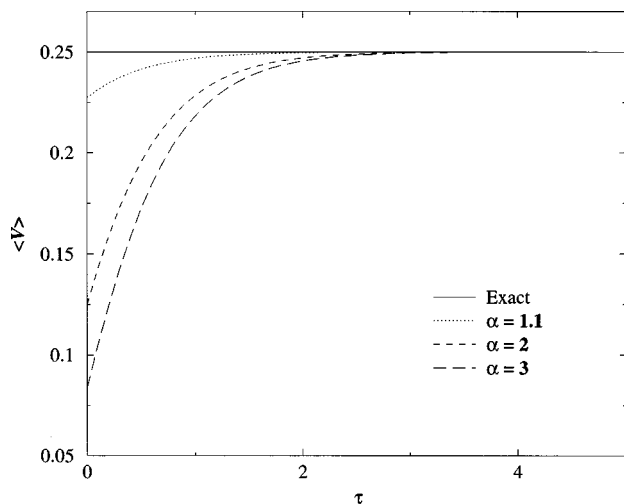


FIG. 4. Evaluation of the average potential energy of the linear harmonic oscillator as a function of propagation time  $\tau$  using the exact propagator [see Eq. (37)] to propagate different wave functions whose form is given by Eq. (46).

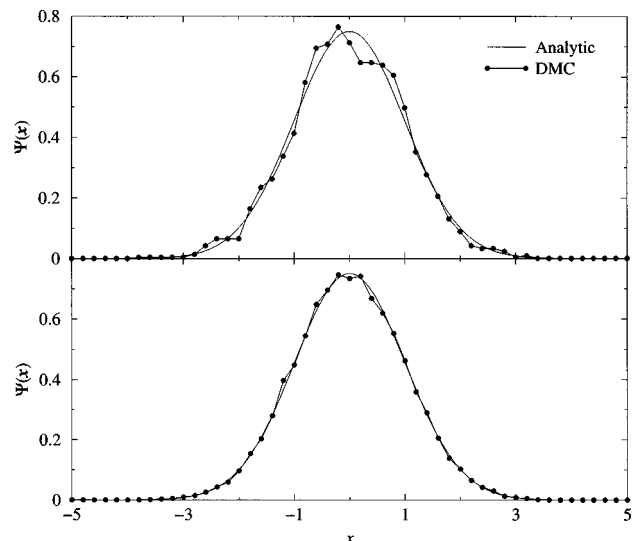


FIG. 5. Spatial distribution of replicas generated by DMC for the linear harmonic oscillator. The upper panel shows one snapshot of 2000 replicas, the lower panel shows twenty snapshots averaged. The solid line shows the exact ground state wave function.

here. The results indicate that as the deviations of the trial function from the exact ground state wave function increase, the imaginary time propagation required to obtain a result within a given tolerance also increase. Comparison of Figs. 3 and 4 shows that the error generated by using a larger initial time step in the first split of the propagator introduces *very small* amplitude contributions from excited states. Thus the imaginary time needed to obtain converged results is shorter than is required if the exact propagator is used together with a trial function that deviates considerably from the true wave function. In other words, having a small error in the propagator but using the ground state wave function is advantageous over propagating exactly a trial function which is a superposition of several eigenstates. This realization provides the basis for the PI-DMC method which approximately propagates a trial wave function that is very close to the ground state wave function.

Up to this point all the results presented are based on analytically derived propagators. We now test the PI-DMC method for the linear harmonic oscillator. A DMC run with a time step of  $\Delta\tau_{\text{DMC}}=0.01$  is performed for 10 000 initial steps, and 10 000 observation steps and of the replicas are stored every 500 steps. The number of replicas is initially set to 2000. Subsequently, open chain path integral Monte Carlo simulations are performed such that the positions of the terminal beads are sampled from the positions of the replicas that were stored during the DMC run. Since there are 20 sets of replicas stored, 20 path integral simulations are performed, and the results are averaged over the 20 runs. The number of equilibration and observation steps is 100 000 and an observation is made every 10 steps. The neighbor list cutoff distance was  $R_{\text{cut}}=0.2$ . We vary two parameters in the path integral runs, the time of propagation, and the discretization. First we use an evenly discretized path integral chain.

In Fig. 5 we compare the histogram of the DMC wave function to the analytic form of the ground state wave func-

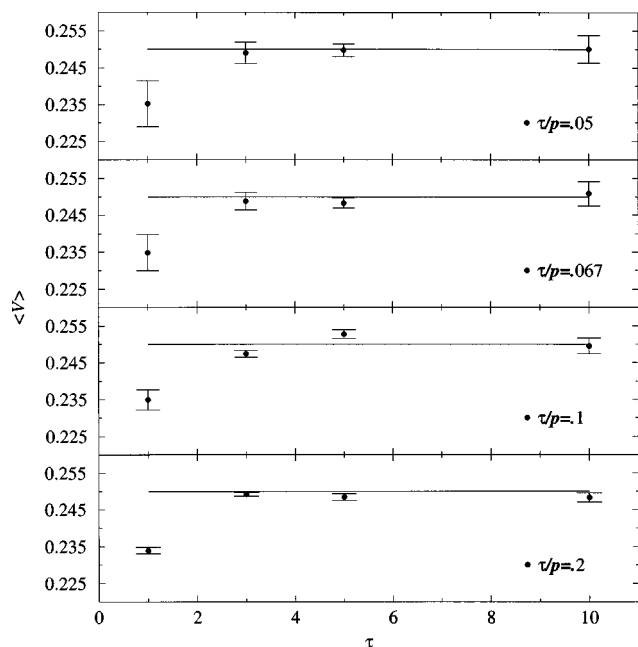


FIG. 6. Evaluation of the average potential energy of the linear harmonic oscillator as a function of propagation time  $\tau$  using the PI-DMC method for four different values of the Trotter parameter  $p$  for the case of even discretization. The solid line shows the analytic result.

tion. The upper panel shows a histogram of replicas (2000 of them) obtained at the end of a DMC run. It compares reasonably with the analytic wave function, but there are some discrepancies. However if we histogram all twenty snapshots we obtain a more precise estimate of the ground state wave function (lower panel). Each snapshot is a starting point of an open chain path integral propagation. Since a single snapshot deviates from the ground state wave function, it is expected that some imaginary time propagation is necessary to determine a ground state observable.

In Fig. 6 we show the average potential calculated by PI-DMC for four imaginary times ( $\tau=1$ ,  $\tau=3$ ,  $\tau=5$ , and  $\tau=10$ ). The virial estimator for the kinetic energy equals the potential energy in this case, therefore we will show only the results for the potential energy. The results in each panel differ in the Trotter discretization used. The data show that upon increasing the time of propagation and the discretization the result converges from below to the known result which is  $\langle V \rangle = 0.25$  (solid line). Varying the discretization turned out to be more relevant, since on the top panel only the shortest run ( $\tau=1$ ) deviates from the known result significantly. As the time of propagation is increased, the error bars of long compared to intermediate imaginary time propagations increase as well. This is expected, since as the propagation time is increased, the polymer used by PIMC lengthens.

Although an observable for this example may be calculated using an evenly discretized propagator, it is still instructive to run a test where the propagator is unevenly discretized. We run a DMC simulation the same way as before. We generate the time steps  $\{\tau_i\}$  according to the recursion formula [Eq. (45)] using input parameters  $a=2$  and  $\delta=0.05$ . The neighbor list cutoff distance in this simulation was  $R_{\text{cut}}$

TABLE I. Evaluation of the average potential of the linear harmonic oscillator as a function of imaginary time  $\tau$  by the PI-DMC method. The initial time step  $\tau_1=0.125$ , other relevant parameters are  $a=2, \delta=0.05$ .

$p$	$\tau$	$\langle V \rangle$
5	0.3375	$0.249 \pm 0.002$
10	0.5875	$0.248 \pm 0.008$
15	0.8375	$0.250 \pm 0.011$

$= 1$ . In Table I we show the result of three propagations where  $\tau_1$  had been set to 0.125 and the number of beads is  $p=10, 20$ , and 30. The results in Table II were generated the same way, except for the fact that the initial time step was set to 0.25. We see that the results are very close to the exact value of 0.25 (this value is always within the error bar). The overall imaginary time  $\tau$  is relatively small in all six cases, which demonstrates the advantage of using the ground state wave function in the propagation.

## B. Double well

In this subsection we present results for a quartic double well potential of the form

$$V(x) = \frac{d}{4} \left( x^2 + \frac{c}{d} \right)^2 - cx^2, \quad (47)$$

where we set  $c=0.15$  and  $d=0.01$ . The simulation details are the same as for the previous example. We compare our results to an imaginary time grid propagation done according to a method developed by Kosloff.<sup>24</sup> Since we are dealing with a one-dimensional system it is instructive to make a comparison of our proposed method to a grid method. Grid methods in general are known to work well in low dimensional systems.

As before a DMC run of 10 000 steps without taking measurements and 10 000 steps such that a configuration is stored every 500 steps is performed. Using the 20 initial configurations generated by DMC, we perform 20 imaginary time PIMC runs using an even breakup of the propagator. Each run equilibrates for 100 000 steps and observations are made every 10 steps for 100 000 steps. The neighbor cutoff distance is  $R_{\text{cut}}=0.1$ .

In Figs. 7 and 8 we show the kinetic and potential energies. The virial estimator has been used to evaluate the kinetic energy. The results indicate convergence as a function of  $\tau$ , and as a function of  $p$ . The results for the total ground state energy using the primitive estimator indicate convergence as well (see Fig. 9).

TABLE II. Evaluation of the average potential of the linear harmonic oscillator as a function of imaginary time  $\tau$  by the PI-DMC method. The initial time step  $\tau_1=0.25$ , other relevant parameters are  $a=2, \delta=0.05$ .

$p$	$\tau$	$\langle V \rangle$
5	0.5375	$0.249 \pm 0.002$
10	0.7875	$0.250 \pm 0.005$
15	1.0375	$0.250 \pm 0.007$

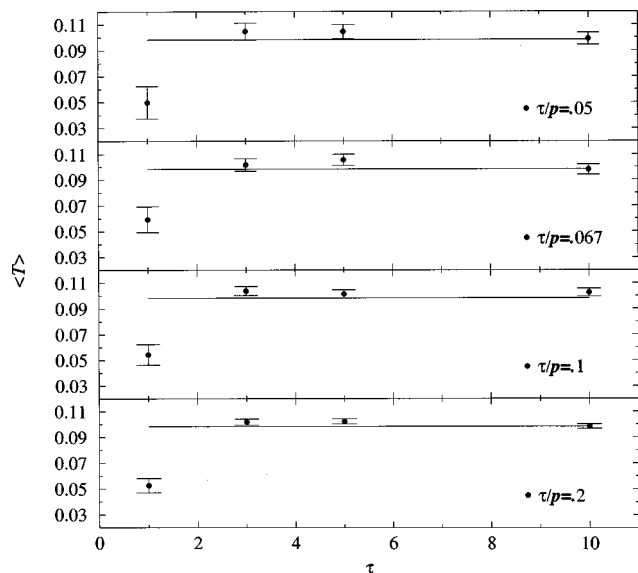


FIG. 7. Evaluation of the average kinetic energy of the one dimensional double well [see Eq. (47)] as a function of propagation time  $\tau$  using the PI-DMC method for four different values of the Trotter parameter  $p$  for the case of even discretization. The solid line shows the result of imaginary time grid propagation. The kinetic energy in the PIDMC results has been estimated using the virial theorem [see Eq. (31)].

### C. Ten-dimensional harmonic oscillator

In the following, we test the method for a model system with many degrees of freedom for which we know the exact result. This system is a set of ten coupled harmonic oscillators with randomly generated frequencies and coupling constants. The Hamiltonian of the system may be written as

$$H = \sum_{\alpha=1}^{10} \left( \frac{P_{\alpha}^2}{2m} + \frac{1}{2} \omega_{\alpha}^2 x_{\alpha}^2 + \sum_{\beta=1}^{10} g_{\alpha\beta} x_{\alpha} x_{\beta} \right). \quad (48)$$

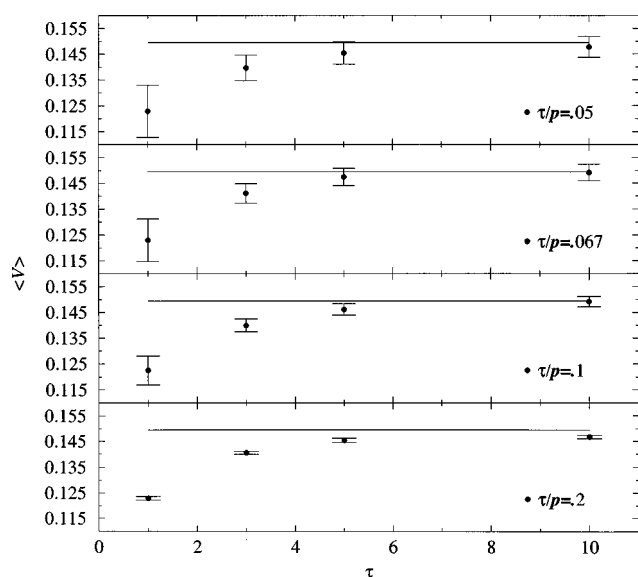


FIG. 8. Evaluation of the average potential energy for the one dimensional double well [see Eq. (47)] as a function of propagation time  $\tau$  using the PI-DMC method for four different values of the discretization parameter  $p$ . The solid line shows the result of numerical imaginary time grid propagation.

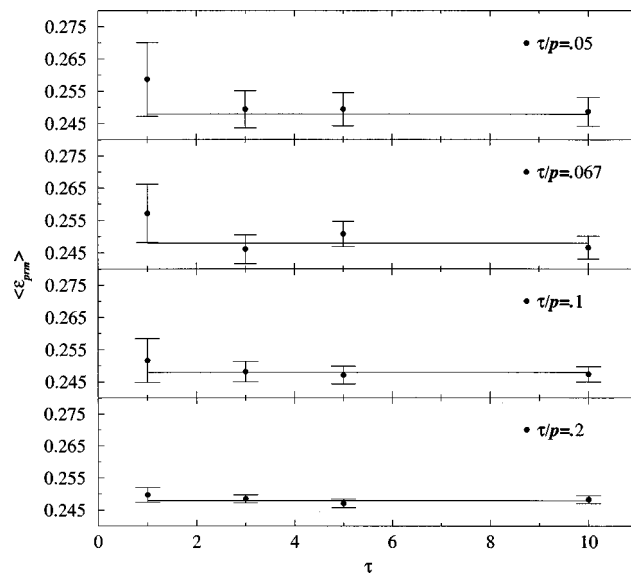


FIG. 9. Evaluation of the average total energy for the one dimensional double well [see Eq. (47)] as a function of propagation time  $\tau$  using the PI-DMC method for four different values of the discretization parameter  $p$ . The primitive estimator of Eq. (36) has been used. The solid line shows the result of numerical imaginary time grid propagation.

The frequencies were kept between 0.6 and 0.7 since if the spread in frequencies is too large, then a multiple imaginary time scale algorithm would have to be introduced. This modification, although certainly possible, shall be the subject of future research. We note in passing that this modification is not necessary for more realistic systems such as a Lennard-Jones clusters. The coupling constants were generated according to

$$g_{ij} = 0.25 \omega_i \omega_j, \quad (49)$$

where  $g_{ij}$  is the coupling constant between mode  $i$  and  $j$ , and  $\omega_i$  is the frequency of mode  $i$ .

We ran a DMC simulation of this system that used 4800 replicas for 10 000 steps. This was enough for the distribution of replicas to reach steady state. Subsequently we ran for 10 000 steps storing a set of replicas every 500 steps and the energy was calculated at every step and averaged. As for the imaginary time PIMC run, we used the 20 stored DMC replicas to perform 20 runs with 10 000 steps equilibration and 10 000 steps for making measurements every 10 steps. The neighbor list cutoff was set to  $R_{\text{cut}} = 0.17$ . For this example we used an uneven breakup of the chain constructed such that the initial imaginary time step  $\tau_1 = 0.9$ , which determines the spring constant between the terminal beads and the beads closest to the terminal beads. Subsequently, each imaginary time slice is determined by the recursion relation Eq. (45).  $\delta$  for each run was set to 0.05. The exact result for the total energy of this system may be obtained by diagonalization and it is  $E_{\text{exact}} = 3.03363$ .

We test the method for three different values of  $a$  ( $a = 3, 2, 1.5$ ) and for each  $a$  four different chain lengths ( $p = 25, 50, 75, 100$ ). The results for the total energy of the system are shown in the set of Tables III–V. We test both the primitive and the virial estimator. Since the virial estimator is a coordinate dependent observable (for the system under

TABLE III. Comparison of the ground state energies a system of ten coupled harmonic oscillators obtained by the PI-DMC method. The parameters for generating the time steps are  $\tau_1=0.9, \delta=0.05, a=3$ .

$p$	$\tau$	$\langle \varepsilon_{\text{vir}} \rangle$	$\langle \varepsilon_{\text{pim}} \rangle$	$\langle E \rangle_{\text{DMC}}$
25	2.40	$2.90 \pm 0.01$	$3.01 \pm 0.02$	$3.04 \pm 0.02$
50	3.65	$2.98 \pm 0.04$	$3.07 \pm 0.03$	...
75	4.90	$2.97 \pm 0.06$	$3.03 \pm 0.04$	...
100	6.15	$3.00 \pm 0.07$	$3.02 \pm 0.04$	...

investigation the ground state energy is twice the potential), it is a valid test of the ability of the method to calculate coordinate dependent observables for quantum many body problems. The rightmost column shows the results for the energy calculated by the DMC run which generated the trial wave function.

The results indicate quantitative agreement. Increasing  $\tau$  seems to have two effects. One is that the expectation values converge to the DMC result, and the other is that the error bars increase. The growth in error bars is expected since as the polymer chain is longer. The fact that the average potential is slightly underestimated is most likely due to the fact that we are using a discretized representation of the path integral. As we have shown using the analytic formula for the discretized imaginary time propagator of the harmonic oscillator that even if the *exact* ground state wave function is used as a trial function and is propagated in imaginary time using a discretized propagator, the average potential is slightly lower than the exact result.

#### IV. CONCLUDING REMARKS

In this paper we have proposed and tested a method for calculating ground state position dependent observables of quantum many body systems. Although we have calculated only the potential, kinetic, and total energies, the procedure is applicable to any observable that can be written in a form that is diagonal in the coordinate representation (order parameter, many body correlation functions, etc.). In our method a PIMC simulation propagates in imaginary time an initial distribution determined by DMC. The use of a DMC wave function is advantageous, because a distribution generated by a DMC will not deviate much from the exact ground state wave function, so short propagation times or equivalently a small PIMC polymer chain will suffice for obtaining accurate values of ground state position dependent observables.

Implementation of the method requires the generalization of the staging algorithm to variable time slices or

TABLE IV. Comparison of the ground state energies a system of ten coupled harmonic oscillators obtained by the PI-DMC method. The parameters for generating the time steps are  $\tau_1=0.9, \delta=0.05, a=2$ .

$p$	$\tau$	$\langle \varepsilon_{\text{vir}} \rangle$	$\langle \varepsilon_{\text{pim}} \rangle$	$\langle E \rangle_{\text{DMC}}$
25	2.24	$2.94 \pm 0.01$	$3.00 \pm 0.02$	$3.04 \pm 0.02$
50	3.99	$2.97 \pm 0.04$	$3.00 \pm 0.03$	...
75	5.24	$2.99 \pm 0.06$	$3.02 \pm 0.03$	...
100	6.49	$2.99 \pm 0.07$	$3.04 \pm 0.04$	...

TABLE V. Comparison of the ground state energies a system of ten coupled harmonic oscillators obtained by the PI-DMC method. The parameters for generating the time steps are  $\tau_1=0.9, \delta=0.05, a=1.5$ .

$p$	$\tau$	$\langle \varepsilon_{\text{vir}} \rangle$	$\langle \varepsilon_{\text{pim}} \rangle$	$\langle E \rangle_{\text{DMC}}$
25	3.44	$2.96 \pm 0.01$	$2.99 \pm 0.02$	$3.05 \pm 0.02$
50	4.69	$2.97 \pm 0.04$	$3.01 \pm 0.02$	...
75	5.94	$2.98 \pm 0.05$	$3.00 \pm 0.03$	...
100	7.19	$3.00 \pm 0.07$	$3.04 \pm 0.04$	...

equivalently variable spring constants for each harmonic bond. This enables control of the acceptance probability of the terminal beads, and control over the convergence of the observables. We have also introduced a neighbor list to sample efficiently the moves for the terminal beads. The generalization of the staging algorithm and the neighbor list are essential for the method to work.

The results for systems of low dimensionality generated by the new method agree well with analytical results or results generated by alternate methods applicable to low dimensional systems. The method also works well for the higher dimensional systems tested in this work. In the future we will assess the efficiency of the new method on large many-body systems of physical interest. One such system we plan to study is the quantum anisotropic planar rotor model,<sup>25</sup> in which anomalous phase transitions at low temperature have been predicted. Evaluation of the ground state order parameter and its moments will provide insight about this phase transition. We anticipate that the PI-DMC method will work well for many-body systems in which both DMC and PIMC simulations are applicable.

#### ACKNOWLEDGMENTS

E.R. acknowledges the Rothschild and Fulbright foundations for financial support. This work was supported by a grant to B.J.B. from the National Science Foundation. The authors wish to thank David Ceperley for reading the manuscript prior to publication and for helpful suggestions. We also thank David Coker for helpful discussions.

<sup>1</sup>D. M. Ceperley and M. H. Kalos, in *Monte Carlo Methods in Statistical Physics*, edited by K. Binder (Springer, Berlin, 1979), Chap. 4, pp. 145–194.

<sup>2</sup>N. Metropolis, A. W. Rosenbluth, M. N. Rosenbluth, A. M. Teller, and E. Teller, *J. Chem. Phys.* **21**, 1087 (1953).

<sup>3</sup>J. B. Anderson, *J. Chem. Phys.* **63**, 1499 (1975).

<sup>4</sup>J. B. Anderson, *J. Chem. Phys.* **65**, 4121 (1976).

<sup>5</sup>J. B. Anderson, *J. Chem. Phys.* **73**, 3897 (1980).

<sup>6</sup>Z. Liu, Ph.D. thesis, Columbia University, 1993.

<sup>7</sup>M. H. Kalos, *Phys. Rev. A* **2**, 250 (1970).

<sup>8</sup>R. D. Amos, *Adv. Chem. Phys.* **67**, 99 (1987).

<sup>9</sup>P. Sandler, V. Buch, and D. C. Clary, *J. Chem. Phys.* **101**, 6353 (1994).

<sup>10</sup>M. H. Müser and J. Ankerhold, *Europhys. Lett.* **44**, 216 (1998).

<sup>11</sup>B. J. Berne and D. Thirumalai, *Annu. Rev. Phys. Chem.* **37**, 401 (1986).

<sup>12</sup>D. Chandler, in *Liquids, Freezing, and Glass Transition*, edited by D. Levesque, J. P. Hansen, and J. Zinn-Justin (North-Holland, Amsterdam, 1991), Chap. 4, pp. 193–285.

<sup>13</sup>D. M. Ceperley, *Rev. Mod. Phys.* **67**, 279 (1995).

<sup>14</sup>R. P. Feynman and A. R. Hibbs, *Quantum Mechanics and Path Integrals* (McGraw-Hill, New York, 1965).

- <sup>15</sup>P. K. Mackeown, *Am. J. Phys.* **53**, 880 (1985).
- <sup>16</sup>K. S. Schweizer, R. M. Stratt, D. Chandler, and P. G. Wolynes, *J. Chem. Phys.* **75**, 1347 (1981).
- <sup>17</sup>L. S. Schulman, *Techniques and Applications of Path Integration* (Wiley-Interscience, New York, 1981).
- <sup>18</sup>It is customary to call the members of the polymer beads. Throughout the rest of the paper we will adhere to this custom.
- <sup>19</sup>The increase in  $p$  (i.e., the refining of the Trotter factorization) has to be carried out such that  $\epsilon_i \rightarrow 0$  for all  $\epsilon_i$ .
- <sup>20</sup>E. L. Pollock and D. M. Ceperley, *Phys. Rev. B* **30**, 2555 (1984).
- <sup>21</sup>M. E. Tuckerman, B. J. Berne, G. J. Martyna, and M. L. Klein, *J. Chem. Phys.* **99**, 2796 (1993).
- <sup>22</sup>B. H. Bransden and C. J. Joachain, *Introduction to Quantum Mechanics* (Longman Scientific and Technical, New York, 1989).
- <sup>23</sup>M. F. Herman, E. J. Bruskin, and B. J. Berne, *J. Chem. Phys.* **76**, 5150 (1982).
- <sup>24</sup>R. Kosloff, *Annu. Rev. Phys. Chem.* **45**, 145 (1994).
- <sup>25</sup>D. Marx and P. Nielaba, *J. Chem. Phys.* **101**, 4538 (1995).